Electronic and optical properties of InSe and GaSe materials: Ab initio study

Mariam Ahmed Elkasllan, Khulood Alshehhi, Fatima Zraydi, Juwayni Lucman, Alam Saj, Basem Abdel Aziz, Ibrahim Al Ghoul , M. Benkraouda, N. Amrane

Physics Department
United Arab Emirates University, Al-Ain, P.O. Box: 17551, U.A.E.

namrane@uaeu.ac.ae

Abstract

We present first principles calculations of the electronic and optical properties of InSe and GaSe binary semiconductor compounds. Electronic properties (band structure, density of states, electronic charge density) and optical properties (the dielectric function, the refractive index, reflectivity, and coefficient of extinction) are successfully calculated using self-consistent scalar relativistic full potential linear augmented plane wave method (FP-LAPW) within the generalized gradient approximation (GGA). The Perdew–Burke–Ernzerhof (GGA08) generalized gradient approximation was used for the total energy calculations, while the Modified Becke–Johnson (MBJ) was used for the electronic structure calculations since this functional was designed to reproduce as well as possible the exact exchange correlation potential rather than the total energy, and as a result gives significantly improved results such as band gap and electronic structure. We also investigated the electronic properties of the ternary alloy $In_xGa_{1-x}Se$. The virtual crystal approximation (VCA) was adopted to model the alloy. The results are compared with previous calculations and with experimental measurements, we found good agreement with our calculations.

Keywords: band structure, density of states, refractive index.

1. Introduction

The recent interest toward layered semiconductors [1–3] is motivated by their potential impact in nanoelectronics [4–6], due to the joint presence of finite values of band gaps [10,11] and flexibility [7,8]. In particular, while graphene does not have a band gap [9], van der Waals semiconductors enable the devising of nanodevices with outstanding values for the ON/OFF ratio [4]. Moreover, by reducing the thickness, in some cases, the band gap becomes direct, with implications for optoelectronics [10] and photodetection.

An advantage of transition metal dichalcogenides (TMDs) is that there is a wide range of them with different band gaps and electron affinities [11], so that they could be used in heterostructures in such devices as tunnel field effect transistors.

These consist of a vertically stacked metal-chalcogen double layers with covalent bonding within the layers and van der Waals bonding between the layers. Carrier mobilities in InSe are of order 1000-2000 $cm^2/V.s$ [12] , similar to those of black phosphorus as they also have s,p-like band edge states. Recently, the quantum Hall effect was observed in the two-dimensional electron gas in GaSe few layer films [13]. Thus, it is important to understand the electronic structure and the optical properties of InSe and GaSe.

Gallium and indium mono-selenides belong to a vast class of layered semiconductors. They have a significant anisotropy of chemical bonds, within and between the layers, which enables preparation of natural and clean surface with a high optical quality by cleavage. Moreover, a GaSe/InSe heterostructure, fabricated by bringing the surfaces of two semiconductors into direct optical contact, is a semiconductor – insulator – semiconductor (SIS) structure where a layer of oxygen atoms adsorbed from atmosphere acts as a dielectric layer [14].

The rest of the paper is organized as follows. In Section 2, we describe the computational method used in the present work. Results about the electronic properties are presented in Section 3. A Conclusion of the work is given in Section 4.

2. Calculations

Scalar relativistic calculations have been performed using the wien2k code [15,16]. For the exchange correlation potential, we have used the local density approximation (LDA) with a

parameterization of Ceperly-Adler data [17]. The new Full Potential Augmented Plane Wave method of the density functional theory is applied [18,19]. Several improvements to solve the energy dependence of the basis set were tried but the first really successful one was the linearization scheme introduced by Andersen[20] leading to the linearized augmented plane wave (LAPW) method. In LAPW, the energy dependence of each radial wave function inside the atomic sphere is linearized by taking a linear combination of a solution *u* at a fixed linearization energy and its energy derivative $\dot{u}$ computed at the same energy.

$$\Phi_K(r) = \begin{cases} \sum_L [a_L^{\alpha K} u_l^\alpha(r') + b_L^{\alpha K} \dot{u}_l^\alpha(r')]\, Y_L(\hat{r}') r' \langle R_\alpha \\ \Omega^{-\frac{1}{2}} exp(i(k+K).r)\, r \in I \end{cases} \quad (1)$$

Where *r'=r-r*$_\alpha$ is the position inside sphere α with polar coordinates r' and r, **k** is a wave vector in the irreducible Brillouin zone, **K** is a reciprocal lattice vector and u_l^α is the numerical solution to the radial Schrodinger equation at the energy ε. The coefficients $a_L^{\alpha K}$ are chosen such that the atomic functions for all L components match (in value) the PW with K at the Muffin tin sphere boundary. The KS orbitals are expressed as a linear combinations of APWs $\Phi_K(r)$. In 1991 Singh [21] introduced the concept of local orbitals (LOs) which allow an efficient treatment of the semi-core states. An LO is constructed by the LAPW radial functions u and $\dot{u}$ at one energy ε_1 in the valence band region and a third radial function at ε_2.

$$\Phi_{LO}(r) = \begin{cases} \left[a_L^{\alpha,LO} u_{1l}^\alpha(r') + b_L^{\alpha,LO} \dot{u}_{1l}^\varepsilon(r') + c_L^{\alpha,LO} u_{2l}^\alpha(r')\right] Y_L(\hat{r}') r' \langle R_\alpha \\ 0 r \in I \end{cases} \quad (2)$$

Recently, an alternative approach was proposed by Sjöstedt et al [22], namely the APLW+ lo (local orbital) method. Here the augmentation is similar to the original APW scheme but each radial wavefunction is computed at a fixed linearization energy to avoid the non-linear eigenvalue problem. The missing variational freedom of the radial wavefunctions can be recovered by adding another type of local orbitals (termed in lower case to distinguish them from LO) containing u and $\dot{u}$term:

$$\Phi_{lo}(r) = \begin{cases} \left[a_L^{\alpha,lo} u_l^\alpha(r') + b_L^{\alpha,lo} \dot{u}_l^\alpha(r')\right] Y_L(r') r' \langle R_\alpha \\ 0 r \in I \end{cases} \quad (3)$$

It was demonstrated that this new scheme converges faster than LAPW. The APW +lo scheme has been implemented in the wien2k code version [23].

More importantly, Generalized gradient approximations (GGA's) for the exchange-correlation energy has also been incorporated; although the GW approximation is a widely used method to predict quasi particle band gaps, as opposed to density functional theory (DFT), which is only applicable to ground state properties, the large computational effort associated with this method limits GW calculations to rather small systems, , one has to note also that GW and hybrid functionals can result in band gap error on the order of 10–20% compared to experimental data [24]. There are some other interesting techniques such as the time dependent density functional theory (TDDFT) [25], this method has achieved an unprecedented balance between accuracy and efficiency for calculations of the excitation spectra and response of atoms and molecules, Given its simplicity, and the relatively modest CPU cost of this type of calculation. The use of TDDFT is increasing, and it is fast becoming one of the tools of choice to get accurate and reliable predictions for excited-state properties in solid state physics, and chemistry, both in the linear and non-linear regimes.

However, in this article we concentrated on the most common approximation, the GGA which makes non-self-consistent evaluation of the quasi particle self -energy, usually the local-density approximation (LDA) or generalized gradient approximation (GGA) [26], the GGA calculations are performed using a consistent GGA treatment of valence and core electrons.

As the LDA approximates the energy of the true density by the energy of a local constant density, it fails in situations where the density undergoes rapid changes such as in molecules. An improvement to this can be made by considering the gradient of the electron density, the so-called Generalized Gradient Approximation (GGA). Symbolically this can be written as:

$$E_{xc} = E_{xc}[\rho(r), \nabla\rho(r)] \qquad (4)$$

There are several different parameterizations of the GGA. A commonly used functional is the PW91 functional, due to Perdew and Yang [27].

However, in the calculations reported here, we chose the muffin tin radii for Ga and Se to be 2.0 and 1.8 a.u. respectively, and 1.9 for Se. The expansion of the spherical region is developed up to l_{max}=10, while in the interstitial region we have used 1890 plane waves for GaSe and 2302 for InSe. Furthermore, we have used the energy cutoff of $R_{□□}.K_{□□□}$=8 and the maximal reciprocal vector equal to 10. The integrals over the Brillouin zone are performed using the Monkorst-pack special k-points approach [28]. Since calculations of the optical properties require a more dense k-matrix, we have used 1000 k-points in the irreducible Brillouin zone for integration in reciprocal space.

Optical properties of a solid are usually described in terms of the complex dielectric function $\varepsilon(\omega) = \varepsilon_1(\omega) + i\varepsilon_2(\omega)$. The dielectric function is determined mainly by the transition between the valence and conduction bands according to perturbation theory, the imaginary part of the dielectric function in the long wavelength limit has been obtained directly from the electronic structure calculation, using the joint density of states (DOS) and the optical matrix elements. It is expressed as

$$\varepsilon_2(\omega) = \frac{4\pi^2 e^2}{3m^2\omega^2}\sum_{l,n}\int_{BZ}\frac{2}{(2\pi)^3}d^3k|P_{nl}|^2.\delta\left[E_l(k) - E_n(k) - \hbar\omega\right] \quad (5)$$

Where m is the mass and e the electrical charge of the electron, $\Sigma_{l,n}$ means the summation between all the conduction bands (l) and valence bands (n); and P_{nl} expresses the momentum matrix element between l and n. It is given by

$$P_{nl} = \frac{m}{\hbar}\langle nk|\nabla_k H,(k)|lk\rangle \quad (6)$$

Where H(k) is the Hamiltonian, and $\langle nk|, |lk\rangle$ are the k-space wavefunctions. Using the FP-LAPW parameters, we can directly calculate P_{nl}.

The real part of the dielectric function can be derived from the imaginary part by the Kramers-Kronig relationship. The knowledge of both the real and the imaginary parts of the dielectric allows the calculation of important optical functions. In this paper, we also present and analyze the refractive index $n(\omega)$ given by

$$n(\omega) = \left[\frac{\varepsilon_1(\omega)}{2} + \frac{\sqrt{\varepsilon_1^2(\omega)+\varepsilon_2^2(\omega)}}{2}\right]^{\frac{1}{2}} \quad (7)$$

At low frequency (ω=0), we get the following relation:

$$n(0) = \varepsilon^{\frac{1}{2}}(0)$$

To correct the LDA error in the band gaps a constant potential was applied to the conduction band states (using the scissors operator which rigidly shifts the conduction band states) in order to match the calculated band gaps with the experimental data.

3. Results

The structural optimization of the Hexagonal phase of GaSe and InSe was performed by calculating the total energy as function versus volume V. The two-dimensional minimization of the total energy requires that each of the self-consistent calculations is converged, so the iteration process was repeated until the calculated total energy of the crystal converged to less than 1 mRyd. A total of eight iterations was necessary to achieve self-consistency. The equilibrium lattice constants and bulk modulus are calculated by fitting the total energy versus volume according to Murnaghan's equation of state (table 4) [29].

3.1 Electronic properties

Electrons interact with the crystal, and this must express itself in their energies, there is an energy gap in the E = E(k) relation for all k vectors ending on a Brillouin zone. A general relation yields for the energies of the kBZ electron waves

$$E(k_{BZ}) = \frac{(\hbar k)^2}{2m} \pm |U(g)| \quad (8)$$

With U(g) being the Fourier component of the periodic potential for the reciprocal lattice vector g considered. The band gap represents the minimum energy difference between the top of the valence band and the bottom of the conduction band.

The electronic band structures of GaSe and InSe along symmetry lines are shown in figures 1 and 2. The calculated band energy gap at high symmetry points is given in table 1, the bandgap for GaSe is found to be direct and equal to 1.9 eV, and that of InSe about 1.15 eV which is in close agreement with earlier work.

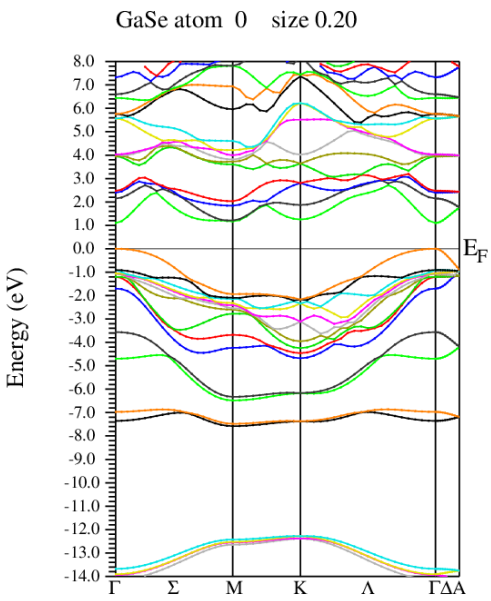

Figure 1. Band structure GaSe.

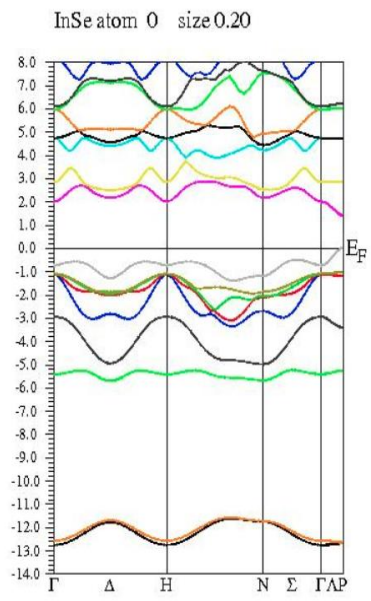

Figure 2. Band structure InSe.

It is found that for the generalized gradient approximation (GGA-2008), the energy gap is underestimated relative to the experimental value due to the well known artifact of the local density approximation calculations, while the Engel-Vosko scheme gives quite a nice band gap compared to the experimental one, the Modified Becke-Johnson (MBJ) gives significantly improved results (see table 1) which is very near the experimental value.

It is interesting to note that quasi-particle excitations are not taken into account in density functional theory (DFT), the energy gap calculated from DFT tends to be smaller than the experimental one. There are several reasons for this. One is that the LDA and GGA functionals contain the self-interaction error and do not show a derivative discontinuity, which is important when one wants to compare the Kohn Sham band gap with the experimental band gap. In some cases, the wrong ground state is found, as, e.g., in Ge, where the band gap is around 0.7 eV, whereas the LDA Kohn-Sham gap is slightly negative at ambient pressure [30]. The GGA approximation yields only a small improvement. Quasiparticle calculations essentially overcome the underestimate of the band gap as obtained using the LDA. The GW calculations for GaN for instance predict band structures in much better agreement with experiment; but they are time

consuming, and also they treat the d valence states as part of the pseudopotential core in the case of GaN.

Table 1. Band energies (eV) for GaSe

	GaSe			
Methods	GGA (2008)	Modified Becke-Johnson	Other method	Experimental
Energy gap (eV)	1.0 eV	1.9 eV	1.7 eV[a]	2.1 eV[b]

Table 2. Band energies (eV) for InSe

	InSe			
Methods	GGA (2008)	Modified Becke-Johnson	Other method	Experimental
Energy gap (eV)	0.7 eV	1.0 eV	1.2 eV[a]	1.1 eV[b]

[a]Reference [31]

[b]Reference [32]

3.2 <u>Optical properties</u>

The study of the optical constants and their variation with frequency is very interesting for the uses of films in optical applications. These applications require accurate knowledge of the optical constants over a wide wavelength range. Extinction coefficient and refractive index. The reflectivity (R) of materials of refractive index (n) and extinction coefficient (k) is given by:

$$R = \frac{(n-1)^2 + k}{(n+1)^2 - k}$$

Tauc et al. [33] and Davis and Mott [34] gave an equation derived independently for the determination of energy band gap nature and the value of Eg (the energy gap) as

$$\alpha(h\nu) = \frac{C}{h\nu}(h\nu - E_g)^m \qquad (12)$$

where m =1/2 for allowed direct transition, m =3/2 for direct ''forbidden'' transition, m =2 for allowed indirect transition and m =3 for indirect ''forbidden'' transition. C is a constant nearly independent on photon energy and known as the disorder parameter. Eg is closely related to energy band gap. Thus, the values of the optical band gap of GaSe and inSe films are obtained by plotting $(\alpha h\nu)^{1/2}$versus $h\nu$ in the high absorption range followed by extrapolating the linear region of the plots to $(\alpha h\nu)^{1/2} = 0$. The analysis of our data showed that plots of $(\alpha h\nu)^{1/2}$ against $h\nu$ give one linear relation which is best fitted by Eq. (9) with m =1/2. This indicates that the allowed direct transition is responsible for interband transition in GaSe and Inse binary compounds, however this preliminary result is not yet reported in this article.

We now turn to the analysis of the optical spectra. The dielectric functions of GaSe and InSe in the Hexagonal structure are resolved into two components $\varepsilon_{xy}(\omega)$, average of the spectra for the

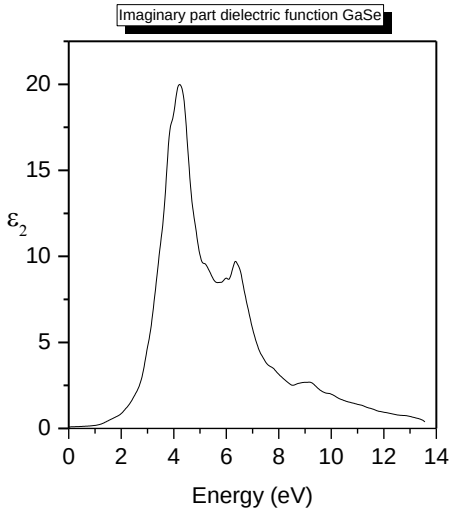

Figure 3a. Imaginary part Dielectric function GaSe.

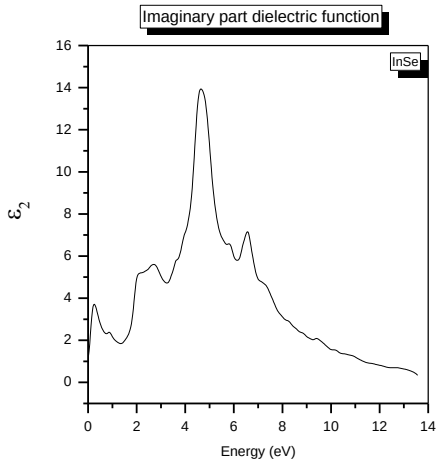

Figure 3b. Imaginary part Dielectric function InSe.

polarization along the x and y-directions and ε_Z, the polarization parallel to the z-direction. The calculated dielectric constants are shown in table 3.

Figures 3a and 3b shows the variation of the imaginary of the electronic dielectric function for GaSe and InSe respectively, for radiation up to 14 eV. The calculated results are rigidly shifted upwards by 1.10 eV . The main feature is a broad peak with a maximum around 5 eV for both compounds and the maximum amplitude is at 16 for GaSe and 11 for InSe, a shoulder is also visible at around 3.8 eV for InSe. The peaks as well as the shoulder are excellently reproduced in the calculations, as are the general form of some experimental spectra. There are also two other groups of peaks, in (7.2 eV- 12.1 eV) photon energy range, they are mainly due to transitions in the vicinity of N. this is usually associated with E_2 transition.

Next, we consider the dispersive part of the dielectric function, ε_1, see figures 4a and 4b. The

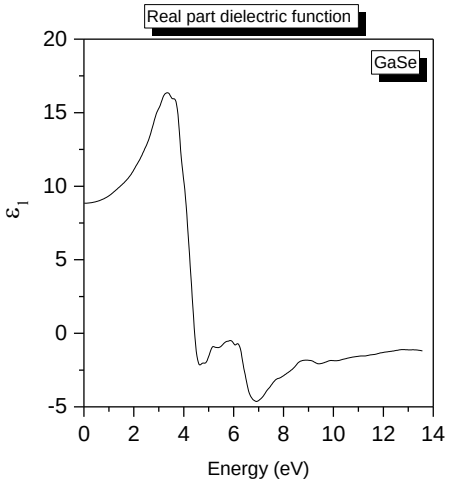

Figure 4a. Real part Dielectric function GaSe.

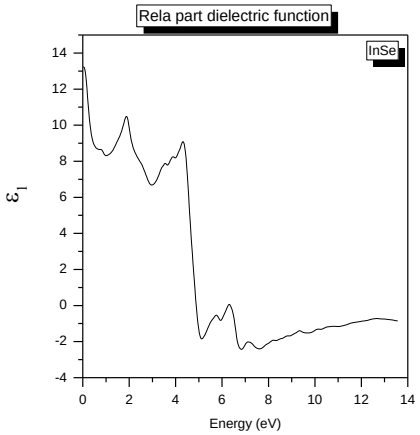

Figure 4b. Real part Dielectric function InSe

calculated spectra have been obtained by Kramers-Kronig transformation of the shifted ε_2 spectra. The main features are a shoulder at lower energies, a rather steep decrease between 3 and 6 eV, after which ε_1 becomes negative, a minimum and a slow increase toward zero at higher energies. The calculated dielectric constants compared with the experimental data and some other work are shown in table 3.

Table 3: The calculated dielectric constants

	$\varepsilon_{\parallel}$		$\varepsilon_{\perp}$	
GaSe	5.64[b]	6.1[a]	6.56[b]	7.44[a]
InSe	6.20[b]	7.6[a]	6.7[b]	7.34[a]
Experiment	---	--	--	--

[a]Reference [35]

[b]Present work

Table 4: Reported and calculated lattice parameters for GaSe and InSe.

Lattice parameters (Å)	GaSe	InSe
Experiment	5.429[a]	5.640[a]
calculated	5.120	5.205
Deviation	0.309	0.435

[a]Reference [36]

We now shortly discuss the spectra obtainable from the dielectric function. As seen in figures 5a and 5b, the refractive index for GaSe and InSe was computed using both real and imaginary

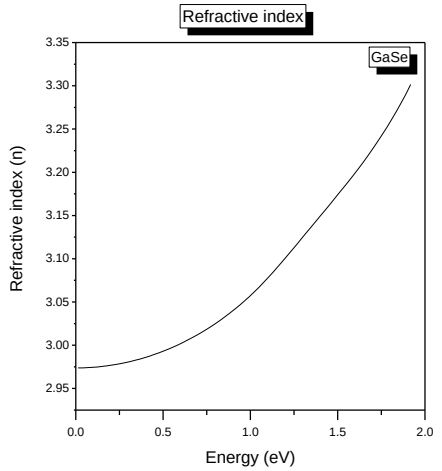

Figure 5a. Refractive index GaSe.

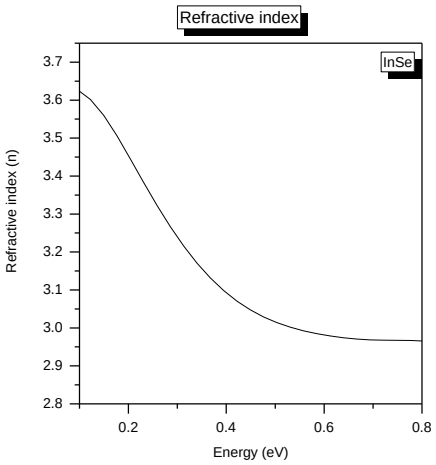

Figure 5b. Refractive index InSe.

parts of the dielectric function. It shows that the refractive index exhibits a significant dispersion in the short wavelength region below λ= 270nm (3.65 eV) where absorption is strong. It decreases with the increase of the energy of the incident light, becoming nearly flat in the higher region. It is observed also that n reached a peak value at 2.55 eV and this peak occurred more or less at the same energy in the real part of the dielectric constant energy dependence curves.

Conclusion

The electronic and optical properties of hexagonal GaSe and InSe semiconductors have been investigated using the wien2k package, full-potential linearized augmented plane wave (FP-LAPW) approach within the density functional theory (DFT) in the local spin density approximation (LSDA) including the generalized gradient approximation (GGA) was used. The use of GGA for the exchange-correlation potential permitted us to obtain good structural parameters. The calculated band-gap was also in good agreement with the other theoretical calculations. The real and imaginary parts of the dielectric functions were calculated for polarization in the x,y plane and along the z-axis, the optical properties are excellently reproduced using the density functional theory, if we allow for a rigid shift of the band structure, the so-called scissors operator.

Acknowledgment

This work was supported by the United Arab Emirates University through the Summer Undergraduate Research Experience (SURE+), Projects: 31S357 and 31S328.

References

[1] Buscema, M.; Island, J.O.; Groenendijk, D.J.; Blanter, S.I.; Steele, G.A.; van der Zant, H.S.J.;

Chem. Soc. Rev. 2015, 44, 3691–3718.

[2] Roldán, R.; Castellanos-Gomez, A.; Cappelluti, E.; Guinea, F. J. Phys. Condens. Matter 2015, 27.

[3] Scholz, A.; Stauber, T.; Schliemann, JPhys. Rev. B 2013, 88.[

[4]Fiori, G.; Bonaccorso, F.; Iannaccone, G.; Palacios, T.; Neumaier, D.; Seabaugh, A.; Banerjee, S.K.; Colombo, L. Nat. Nanotechnol. 2014, 9, 768–779

[5] Koppens, F.H.L.; Mueller, T.; Avouris, P.; Ferrari, A.C.; Vitiello, M.S.; Polini, M.

Nat. Nanotechnol. 2014, 9, 780–793.

[6] Lee, J.Y.; Shin, J.H.; Lee, G.H.; Lee, C.H, Nanomaterials 2016, 6, 193.

[7] Akinwande, D.; Petrone, N.; Hone, J. Nat. Commun. 2014, 5.

[8] Zhu, W.; Yogeesh, M.N.; Yang, S.; Aldave, S.H.; Kim, J.-S.; Sonde, S.; Tao, L.; Lu, N.; Akinwande, D. Flexible, Nano Lett. 2015, 15, 1883–1890.

[9] Novoselov, K. Nat. Mater. 2007, 6, 720–721

[10] Wang, X.; Huang, L.; Peng, Y.; Huo, N.; Wu, K.; Xia, C.; Wei, Z.; Tongay, S.; Li, J. Enhanced rectification, Nano Res. 2015, 9, 507–516.

[11] Gong C, Zhang H J, Wang W H, Colombo L, Wallace R M and Cho K J 2013 Appl Phys Lett 103, 053513. 2015 Appl Phys Lett 107, 139904.

*[12] Sucharitakul S, Goble N J, Kumar U R, Sankar R, Bogorad Z A, Chou F C, Chen Y T and Gao X P A 2015 Nano Lett **15** 3815-9*

[13] Bandurin D A, Tyurnina A V, Yu G L, Mishchenko A, Zólyomi V, Morozov S V, Kumar R K, Gorbachev R V, Kudrynskyi Z R, Pezzini S, Kovalyuk Z D, Zeitler U, Novoselov K S, Patanè A, Eaves L, Grigorieva I V, Fal'ko V I, Geim A K and Cao Y 2016 Nat Nano.

[14] S.I. Drapak, V.B. Orletskii, and Z.D. Kovalyuk, Semiconductors, 38 (2004) 546.

[15] K.Schwarz, P.Blaha, G.K.H.Madsen, Comput.Phys.Commun. 147 (2002) 71

[16] K.Schwarz, P.Blaha, Comput.Mater.Sci. 28 (2003) 259

[17] D.M.Ceperley, B.I.Alder, Phys.Rev.Lett.45 (1990) 566

[18] E.Wimmer, H.Krakauer, M.Weinert, A.J.Freeman, Phys.Rev.B24 (1981) 864

[19] P.Blaha, K.Schwarz, P.Sorantin, S.B.Trikey, Comput.Phys.Commun.59 (1990) 399

[20] O.K.Andersen, Phys.Rev.B12 (1975) 3060-3083

[21] D.Singh, Phys.Rev.B 43 (1991) 6388-6392

[22] E.Sjöstedt, L.Nordström, D.J.Singh, Solid State Comm.114 (2000) 15-20

[23] P.Blaha, K.Schwarz, G.K.H.Madsen, D.Kvanicka, J.Luitz, WIEN2k,An Augmented Plane Wave Plus Local Orbitals Program For Calculating Crystal properties, Vienna University of Technology,Austria 2001.

[24] Yoon-Suk Kim et al, Phys. Rev. B 82 (2010) 205212

[25] A D Zdetsis, C S Garoufalis, M S Skaperda and E N Koukaras Journal of Physics: Conference Series 10 (2005) 101–104

[26] John P. Perdew, Kieron Burke, Matthias Ernzerhof, Phys. Rev.*

Let., Vol. 77, No 18 (1996)

[27] J. P. Perdew, J. A. Chevary, S. Vosko, K. A. Jackson, M. R. Pederson, D. J. Singh, and C. Fiolhais Phys. Rev. B 46, 6671 (1992)

[28] H.J.Monkhorst, J.D.Pack, Phys.Rev.B13 (1976) 5188

[29] Murnaghan F D 1944 Proc. Natl Acad. Sci. USA 30 5390

[30] M.Alouani and J.M.Wills, Phys.Rev.B54, 2480 (1996)

[31] JOURNAL OF OPTOELECTRONICS AND ADVANCED MATERIALS, Vol. 11, No. 6, June 2009, p. 797 – 812

[32] B. Gürbulak, Solid State Commun. ***109,*** *665 (1999).*

[33] J. Tauc, R. Grigorovici, A. Vancu, Phys. Stat. Sol. 15 (1966) 627

[34] N.F. Mott, E.A. Davis, Electronic Processes in Non-

Crystalline Materials, Clarendon Press, Oxford, 1979.

[35] Polian A, Besson J M, Grimsditch M and Vogt H 1982 Phys.Rev. B ***25*** *2767*

[36] V N Brudnyi, S Yu Sarkisov and A V Kosobutsky, Semiconductor Science and Technology, Vol. 30, 11 (2015)